Volume Rendering

Assignment 1 of Visualization

Group 36
Yuhao Cheng (1379879)
Xin Zhao (1329553)

Eindhoven University of Technology

Contents

1 Raycasting **2**
1.1 Trilinear interpolation 2
1.2 Maximum intensity projection 3
1.3 Compositing 4
1.4 Responsiveness 5

2 2D Transfer Function **7**
2.1 Gradient-based opacity weighting 7
2.2 Illumination model 9

3 Data exploration of contest dataset **10**
3.1 Volume fraction of water 10
3.2 Volume fraction of asteroid 11
3.3 Pressure in microbars 12
3.4 Temperature in electronvolt 13

4 Evaluation **16**
4.1 MIP 16
4.2 Compositing 16
4.3 2D transfer function 17

Chapter 1

Raycasting

In this chapter, we explain the methods of linear interpolation, maximum intensity projection, compositing and responsiveness. Also, we show the implementation of these methods on several datasets.

1.1 Trilinear interpolation

Trilinear interpolation computes intensity values for voxels with unknown intensity values, which are located between voxels that have known values. It estimates the value by linearly weighting the 8 closest neighboring values. Figure 1.1 depicts the method of trilinear interpolation. It is used to determine an intensity value at the point (x, y, z), given the values at the 8 corners of the cube as $v_{000}, v_{001}, v_{010}, ..., v_{110}, v_{111}$. The unknown value is computed using the known corner values and their distance from the location of the point (x, y, z) according to the following method:
Firstly, We define d_x as the difference between x and the smaller coordinate related, and we get $d_x = (x - x_0)/(x_1 - x_0)$, where x_0 and x_1 correspond to the points below x and above x, respectively. Also, we can get d_y and d_z using the same way: $d_y = (y - y_0)/(y_1 - y_0)$, $d_z = (z - z_0)/(z_1 - z_0)$, where y_0, y_1, z_0 and z_1 are defined like x_0 and x_1. Then, we implement the interpolation along x,

$$v_{00} = v_{100} * d_x + v_{000} * (1 - d_x) \tag{1.1}$$
$$v_{10} = v_{110} * d_x + v_{010} * (1 - d_x) \tag{1.2}$$
$$v_{01} = v_{101} * d_x + v_{001} * (1 - d_x) \tag{1.3}$$
$$v_{11} = v_{111} * d_x + v_{011} * (1 - d_x) \tag{1.4}$$

where v_{000} is the value of corner (x_0, y_0, z_0), and other 3 points are also defined like this.
Next, we implement the interpolation along y,

$$v_0 = v_{10} * d_y + v_{00} * (1 - d_y) \tag{1.5}$$
$$v_1 = v_{11} * d_y + v_{01} * (1 - d_y) \tag{1.6}$$

Finally, we implement the interpolation along z,

$$v = v_1 * d_z + v_0 * (1 - d_z) \tag{1.7}$$

and we get the value v, which is the value of point (x, y, z) that we want to calculate.

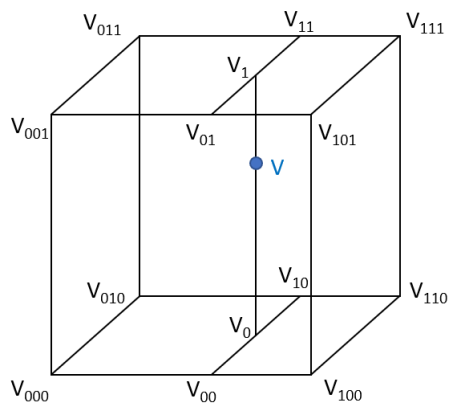

Figure 1.1: Depiction of method of trilinear interpolation

1.2 Maximum intensity projection

Maximum intensity projection (MIP) is a volume rendering technique for 3D dataset. Figure 1.2 depicts the direct volume rendering technique. For each pixel in the 2D image, a ray is shot into the 3D volume data. The maximum value determined by trilinear interpolation along this ray is collected and displayed at the corresponding pixel of the 2D image. After scanning all pixels of the image, we can get the final result of MIP. MIP does not require the generation of color and opacity transfer functions, but display density information. The formula used to determine the value for each pixel is:

$$I(p) = max\{s(t) \mid 0 \leq t \leq 1\} \tag{1.8}$$

where $s(t)$ is the scalar value of voxel and $I(p)$ is the scalar value for pixel p.

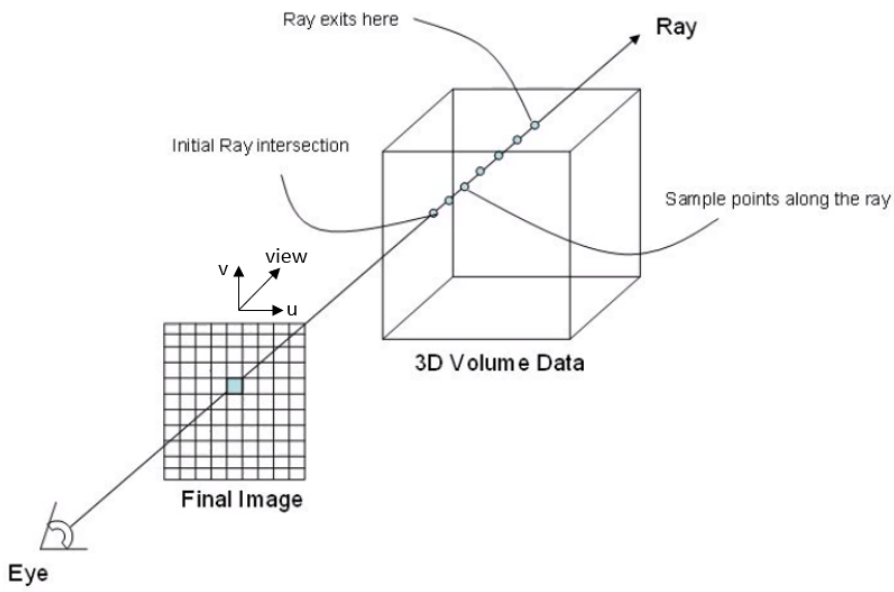

Figure 1.2: Direct volume rendering technique

We implement MIP method on several datasets, the results are shown in Figure 1.3. Figure 1.3(a) shows the inside of a backpack on a basket, We can find two cans, one lighter, a rope and a box inside. Figure 1.3(b) shows the bone structure of the fish clearly. Figure 1.3(c) shows the MIP rendering result of pig dataset, but we cannot see the inside of the pig. Figure 1.3(d) shows MIP rendering result of tomato dataset, but it is difficult to view the tomato and it does not show the seeds inside.

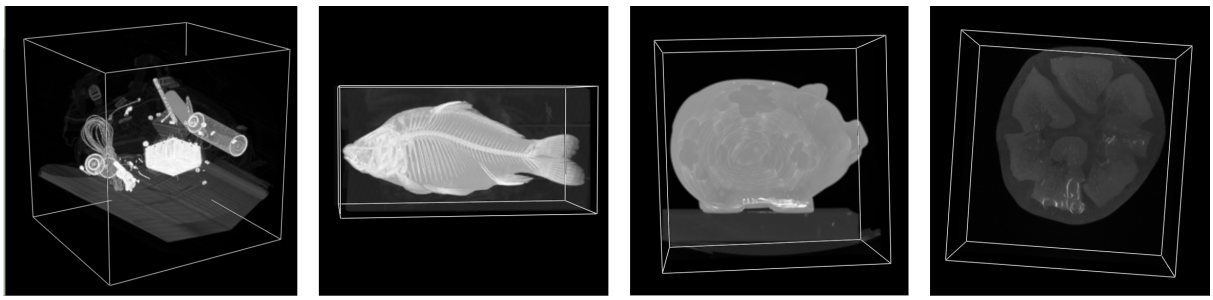

(a) (b) (c) (d)

Figure 1.3: MIP rendering results of several datasets

1.3 Compositing

Compositing method allows us to merge the interpolated colors and opacities with each other to yield the color of the pixel, so that the semi-transparent layers are made

visible. The formula used to determine the value for each pixel is:

$$I(p) = \sum_{i=0}^{n-1} c_i \prod_{j=i+1}^{n-1} (1 - \tau_j) \tag{1.9}$$

where $I(p)$ is the value for pixel p, c_i is the color of voxel i and τ_j is the opacity of voxel j.
We can get the color and opacity of each voxel using 1D transfer function, then we can get the pixel color by applying the following formula in back-to-front order (starting at the background and moving towards the image plane):

$$C_i = \tau_i c_i + (1 - \tau_i) C_{i-1} \tag{1.10}$$

where C_{i-1} and C_i are the calculated pixel colors from background to voxel $i-1$ and voxel i. We use this formula for all the sample points along the current ray to get the pixel color and assign it to the corresponding pixel in the 2D image. After scanning all pixels, we can get the final image.

We applied compositing method on the fish dataset. Figure 1.4(a) shows the skin (pink), bones(white), and the surrounding(yellow) of the fish. On the transfer function panel, the region A, B, C and D represent the noise, surrounding, skin and bones, respectively. Figure 1.4(b) shows the surrounding of the fish by increasing the opacity of yellow color and decreasing the opacity of pink and blue colors. Figure 1.4(c) and figure 1.4(d) shows the skin and bones structure of the fish using the same way as figure 1.4(b).

1.4 Responsiveness

When the program is rendering, it runs quite slow, so we lowers the resolution during rendering. In our program, we set the scanning step of the image to 5 when we interact with the mouse, thus, a square of 5×5 pixels will have the same color, and we set scanning step of the image to 1 when interaction stops. Also, we set the step of sample points along view vector to 5 and 1 with and without interaction with the mouse, so the responsiveness can be enhanced as well. Figure 1.5 (a) and (b) show the compositing image of the pig datasete. When we do not rotate the image, we can clearly see the coins inside the pig, while when we interact with the mouse, the whole image becomes blurry and it is difficult to see the coins.

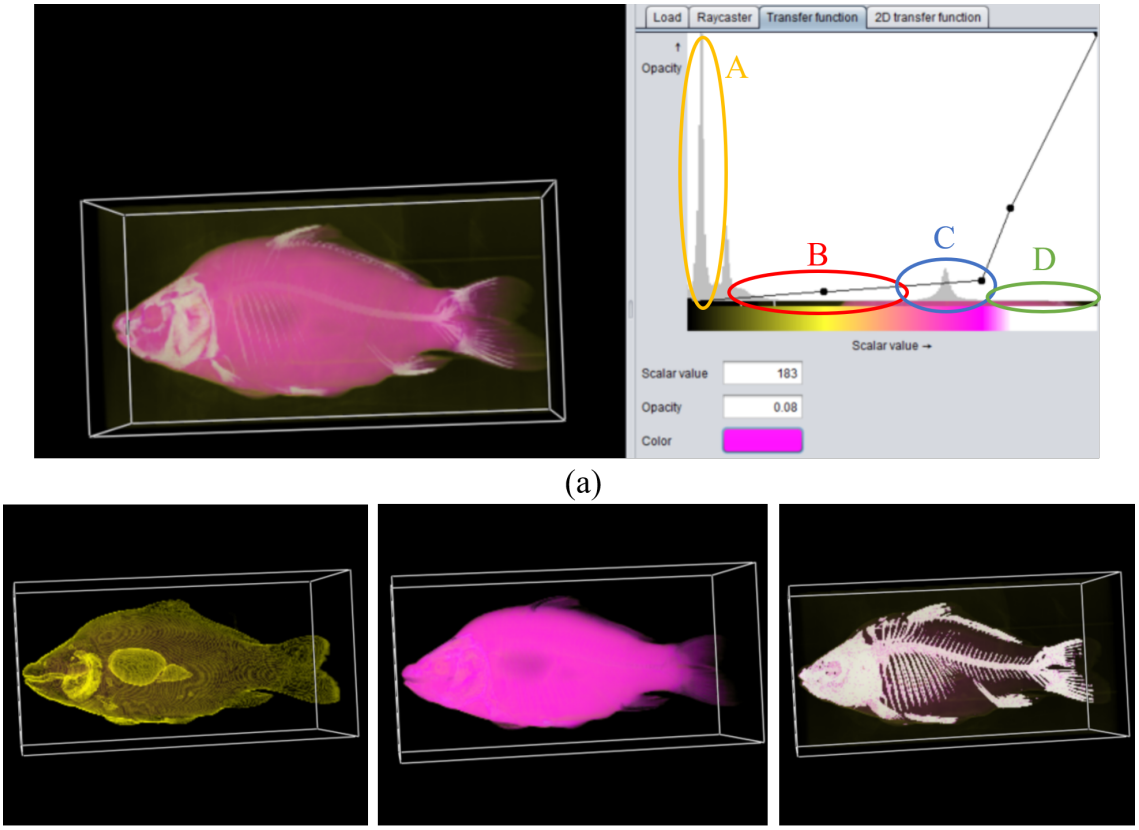

(a) (b) (c) (d)

Figure 1.4: Compositing rendering result of fish dataset

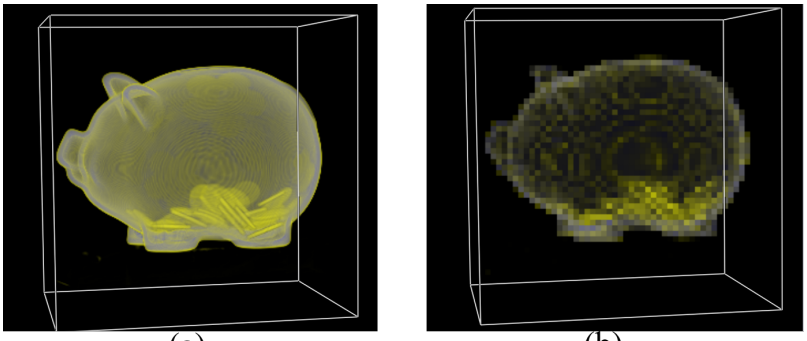

(a) (b)

Figure 1.5: Resolution comparison with and without rotating the image

Chapter 2

2D Transfer Function

In this chapter, we explain the methods of Gradient-based opacity weighting and illumination model. Also, we show the implementation of these methods on several datasets.

2.1 Gradient-based opacity weighting

2D transfer function has two-dimensional domain, with the scalar value on one axis, and gradient magnitude on the other axis. The gradient magnitude is a measure of local rate of change. One reason we used higher dimensional transfer functions is that one-dimensional transfer functions can not accurately capture all material boundaries, even for a clean, high-resolution dataset. In addition, 2D transfer function is very useful to highlight different materials easily when there is a lot of different materials with different voxel values. The user can display and hide certain parts of the scene using this method. Marc Levoy used 2D transfer functions and proposed the following equation to calculate the opacity of each voxel:

$$\alpha(x_i) = \alpha_v \begin{cases} 1, & if\ |\nabla f(x_i)| \ = \ 0\ and\ f(x_i) \ = \ f_v \\ 1 - \frac{1}{r}\left|\frac{f_v - f(x_i)}{\nabla f(x_i)}\right|, & if\ |\nabla f(x_i)| \ > \ 0\ and \\ & f(x_i) - r|\nabla f(x_i)| \leq f_v \leq f(x_i) + r|\nabla f(x_i)| \\ 0, & otherwise \end{cases} \tag{2.1}$$

where α_v is the desired overall opacity, r is the desired thickness of the transition region, f_v is the desired intensity at the center of the transition region, $f(x_i)$ is the intensity of the voxel, and $|\nabla f(x_i)|$ is the gradient magnitude at the voxel. $\nabla f(x_i)$ is the gradient that is approximated by using central differencing method:

$$
\begin{aligned}
\nabla f(x_i) &= f(x_i,\ y_i,\ z_i) \\
&= (\frac{1}{2}((f_{x+1},\ y_j,\ z_k) - (f_{x-1},\ y_j,\ z_k)), \\
&\quad \frac{1}{2}((f_x,\ y_{j+1},\ z_k) - (f_{x-1},\ y_{j-1},\ z_k)), \\
&\quad \frac{1}{2}((f_x,\ y_j,\ z_{k+1}) - (f_{x-1},\ y_j,\ z_{k-1}))).
\end{aligned} \tag{2.2}
$$

then we can use equation 1.10 to get the pixel color.
We applied 2D transfer function to the tooth dataset, and analyzed the three parameters of 2D transfer function: overall opacity, radius and intensity. Figure 2.1(a) shows the image of tooth with default parameters (opacity=0.3, radius=1.752, intensity=646)). In figure 2.1(b), we change the overall opacity from 0.3 to 0.8, the surface becomes more opaque and it is difficult to see the inside of the tooth. In figure 2.1(c), we change the radius from 1.752 to 0.374, then we find that the image lose a lot of shading points. In figure 2.1(d), we change the intensity from 646 to 999, then the image does not show the root of the tooth any more, it only shows the head of the tooth with more details than figure 2.1(a).

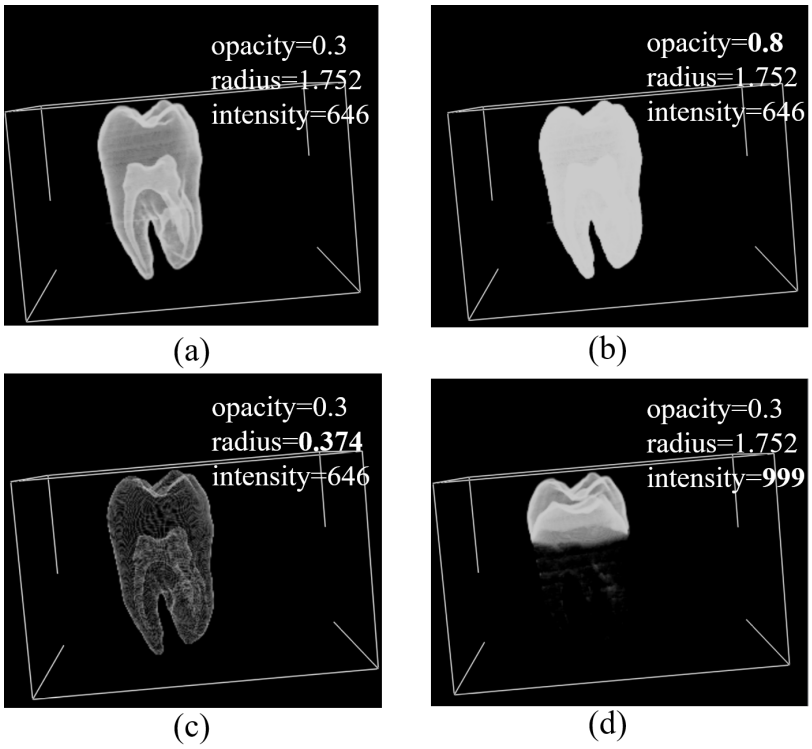

Figure 2.1: Applying 2D transfer function to the tooth dataset

2.2 Illumination model

We implement the Phong shading model on our program, which can be used in the method of compositing and transfer 2D function. This model includes three parts, ambient part, diffuse part and specular part, the formula of Phong shading model is shown below:

$$I = I_a k_{ambient} + I_I k_{diff}(L \cdot N) + I_I k_{spec}(V \cdot R)^{\alpha} \tag{2.3}$$

where $k_{ambient}$ is the ratio of reflection of the ambient term, k_{diff} is the ratio of diffuse reflection term of incident light, k_{spec} is the specular reflectance of incident light, α is a shininess constant for this material, V is the normalized view vector, N is the normalized gradient vector, L is the vector from the point on the surface toward light source, and R is the reflection vector.

We applied compositing and shading method on the bonsai dataset. Figure 2.2(a) and Figure 2.2(b) show the rendering results without and with shading. After using shading method, the image becomes more stereoscopic. We set the paramers of figure 2.2(b) as the default parameters($K_{ambient} = 0.1$, $k_{diff} = 0.7$, $k_{spec} = 0.2$), then we change the values of $K_{ambient}$, k_{diff}, k_{spec} to see the difference. For figure 2.2(c) and figure 2.2(d), we changed the value of $K_{ambient}$ as 0.4 and 0.7. When $K_{ambient}$ changes from 0.1, 0.4 to 0.7, the whole image becomes brighter. For figure 2.2(e) and figure 2.2(f), we changed the value of K_{diff} as 0.1 and 0.4. When K_{diff} changes from 0.1, 0.4 to 0.7, the intensity of diffuse light increases and the image becomes clearer. For figure 2.2(g) and figure 2.2(h), we changed the value of K_{spec} as 0.4 and 1. When K_{spec} changes from 0.2, 0.4 to 1, the reflected light becomes stronger.

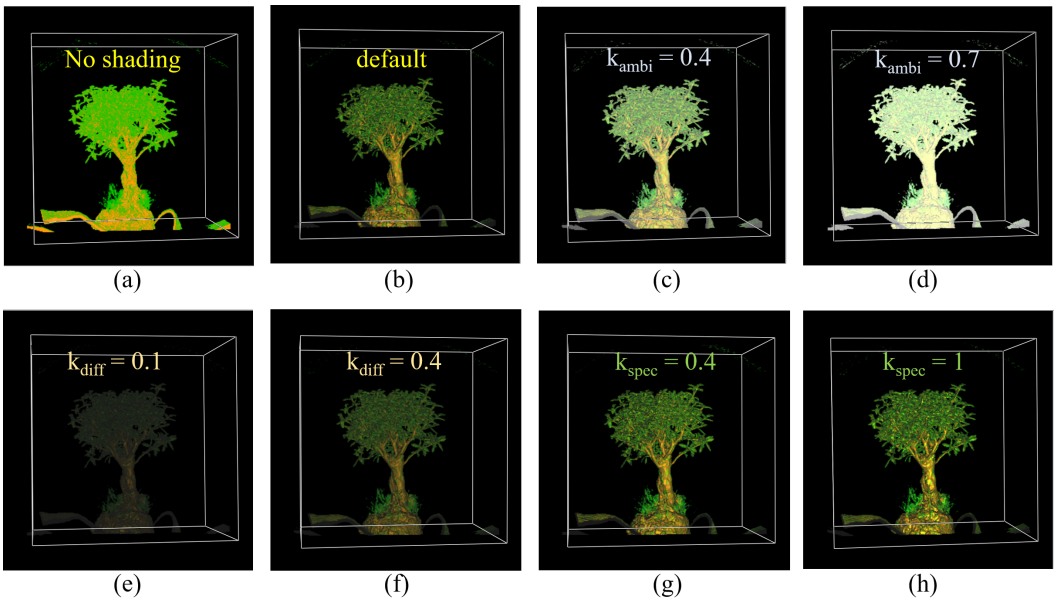

Figure 2.2: Applying compositing and shading method to the bonsai dataset

Chapter 3

Data exploration of contest dataset

In this chapter, we show the data exploration results of the contest data. Different techniques are applied to several datasets, and a lot of details and explanation of the rendering results are shown.
The contest dataset have two groups and 4 kinds of data, including v02 (volume fraction of water), v03 (volume fraction of asteroid), prs (pressure in microbars), and tev (temperature in electronvolt). The time interval of group yB31 is larger than yA31, so we use group yB31 to show the evolution of data. Also we can compare the difference between yA31 and yB31 by comparing data in time 39924 of yB31 and data in time 39803 of yA31, because these two time points are very close.

3.1 Volume fraction of water

Firstly, we show the evolution of water volume of group yB31. We applied compositing method on these dataset and the results are shown in figure 3.1(a)-(e). The transfer function is shown in the subgraph of figure 3.1(a), and the numbers of parameters of transfer function are explained in the figure caption. In figure 3.1(a), asteroid impacts the water and creates a cavity on the surface of water. As time goes by, more energy is transferred from asteroid to water, thus, a large amount of water travels along the entry corridor of the asteroid, and then a lot of water rises into the air and height of the splash increases.
We also compared the water volume in time 39924 of group yB31 (figure 3.1(d)) with water volume in time 39803 of group yA31 (figure 3.1(f)). We can see that yA31 has a larger water splash than yB31, which indicates that more kinetic energy is transferred to the water in yA31. Based on this observation, we conclude that yA31 has more possibilities to generate a threat of tsunamis and have stronger influence on the climate due to more water vapor entering the atmosphere.

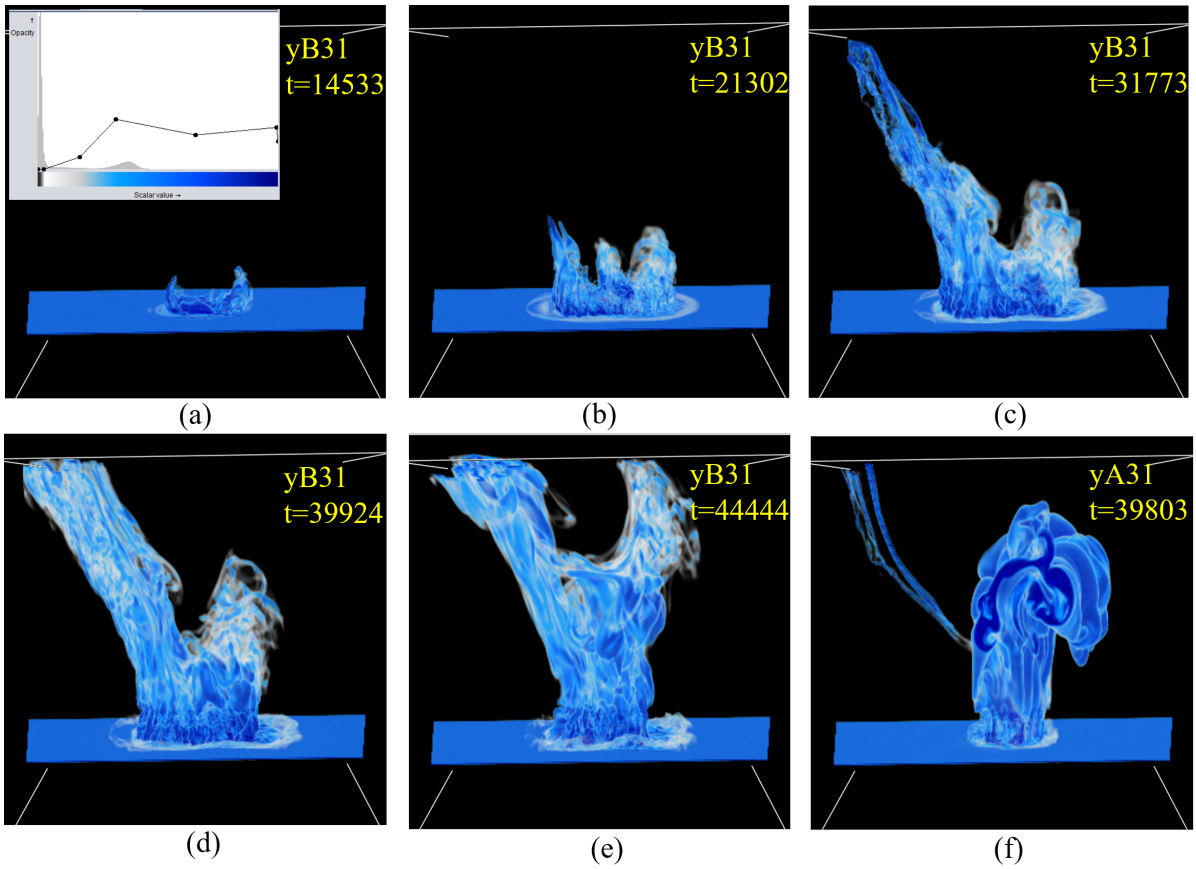

Figure 3.1: Rendering results of volume fraction of water at different time and different group of datasets. Figure 3.1(a)-(e) are generated from yB31, and Figure 3.1(f) is generated from yA31. The transfer function used in these six figures is shown in the subgraph of figure 3.1(a), the parameters of points are shown as following: (0, 0, 0, 0, 0), (5, 1, 1, 1, 0), (36, 0.8, 0.8, 0.8, 0.08), (67, 0, 0.64, 1, 0.32), (135, 0, 0.3, 1, 0.22), (204, 0, 0, 0.51, 0.27), (255, 0, 0, 0.74, 0.18), with the five numbers correspond to intensity, R, G, B and opacity.

3.2 Volume fraction of asteroid

We use the same method as the water volume to show the evolution of asteroid volume. Figure 3.2(a)-(e) shows the evolution of asteroid volume of group yB31, figure (f) shows the asteroid volume in time 39803 of yA31. In figure 3.2(a), there is a tail of asteroid in the atmosphere, we think it is due to the air friction causing the asteroid to decay, leaving the asteroid material in the air. When the asteroid impact the water, it produces an explosion, and the asteroid is driven apart. As time goes by, most material of asteroid raises to the atmosphere and spread a very large volume.
We also compared the asteroid volume in time 39924 (figure 3.2(d)) with that in time 39803 (figure 3.2(f)). It is clear that there are more materials of asteroid in the atmosphere in yB31 than yA31. Considering the rending images of water volume, we know that the asteroid in yA31 transfers more energy into water, thus, there are more volume

of water and less volume of asteroid rised to the air in yA31.

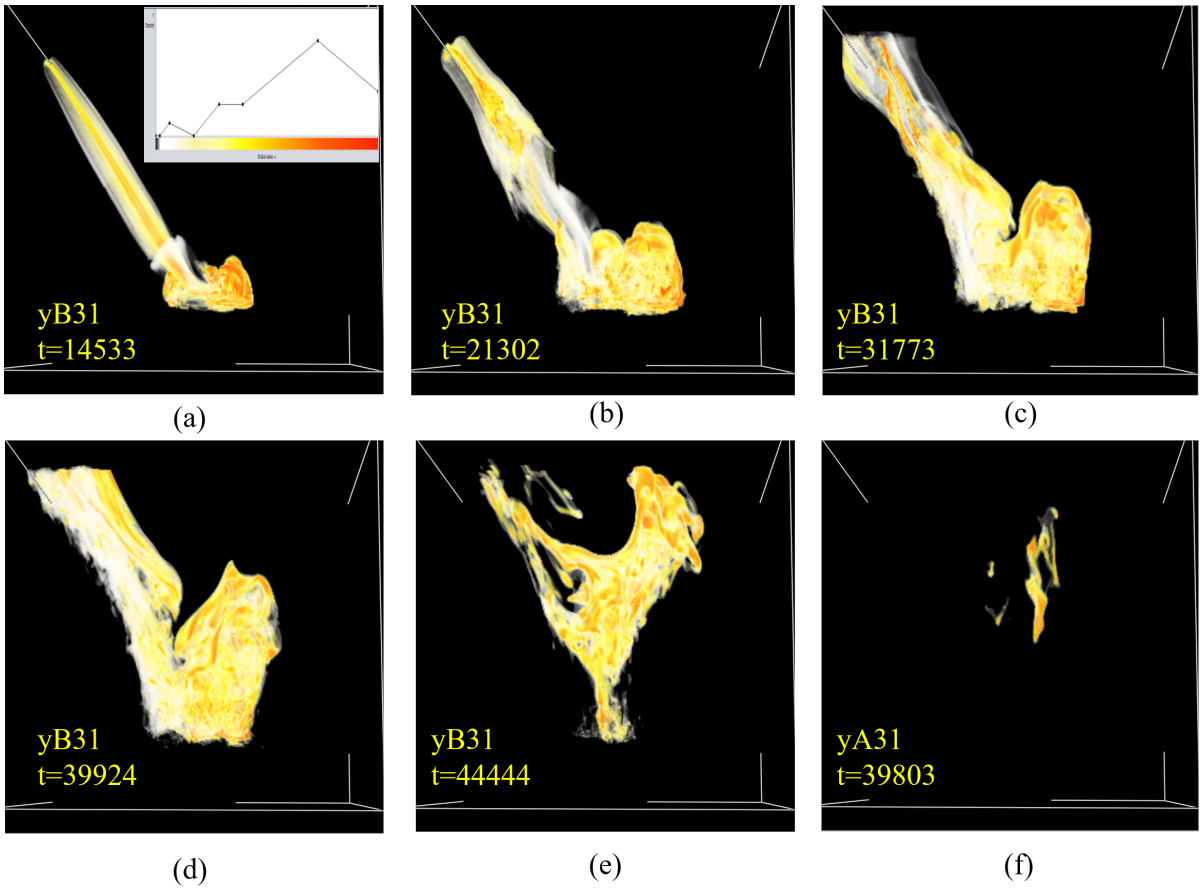

Figure 3.2: Rendering results of volume fraction of asteroid at different time and different group of datasets. Figure 3.2(a)-(e) are generated from yB31, and Figure 3.2(f) is generated from yA31. The transfer function used in these six figures is shown in the subgraph of figure 3.2(a), the parameters of points are shown as following: (0, 0.0, 0.0, 0.0, 0.0), (5, 1, 1, 1, 0.0), (16, 1, 1, 1, 0.1), (44, 1, 0.94, 0.678, 0.0), (73, 1, 1, 0.6, 0.25), (100, 1, 1, 0, 0.25), (186, 1, 0.4, 0, 0.75), (255, 1.0, 0.137, 0, 0.35), with the five numbers correspond to intensity, R, G, B and opacity.

3.3 Pressure in microbars

In this secton, we applied MIP, compositing and 2D transfer function to prs dataset, and compare the difference of results when using compositing and 2D transfer function.
Firstly, we use the MIP method to analyze the pressure at time 14533 and 21302 of group yB31. Figure 3.3(a) and (b) show the MIP rendering results. From the cross section of water, we can see that the color changes from black to white as the depth of water increases, which means the pressure increases as the depth increases. At time 14533 when the asteroid just impacts the water, we can see a arc-shaped pressure wave in center of the water, and it corresponds to the place where the pressure is the highest.

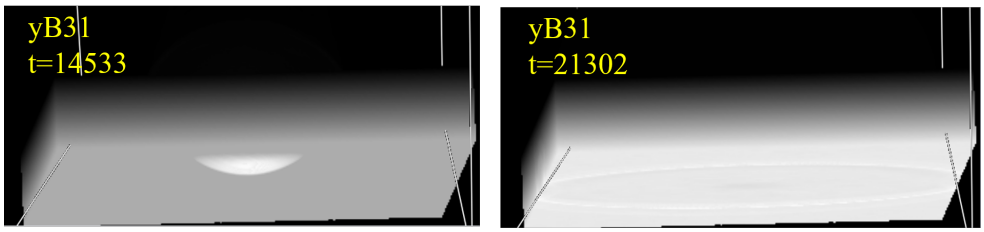

(a) (b)

Figure 3.3: Rendering results of pressure at time 14533 and 21302 using MIP

At time 21302, the pressure wave propagates around and generates a larger circle, and the distribution of pressure becomes more uniform.
Then, we use compositing and 2D transfer function to analyze the pressure at time 14533 of group yB31, and compare the two methods by observing the rendering results. Figure 3.4(a) and (b) show the rendering results at time 14533 using compositing and 2D transfer function. In figure 3.4(b), we can see that the shape of the pressure wave is round shape on the right side and not uniform on the left side. However, it is difficult to see these information in figure 3.4(a). Hence, it is very clear that using 2D transfer function can show more boundary information than the 1D transfer function. The reason why the pressure wave is round shape on the right side but not uniform on the left side, is that the pressure wave generated at the surface of water will move from left to right. We get this conclusion according to rendering image of water and asteroid. Since we know that the asteroid impacts the water at nearly 45 degrees from left to right, therefore, after the asteroid impacts the water, the pressure wave will move to the right.
Finally, we applied 2D transfer function on yB31 dataset at time 14533, and studied the pressure conditions at different depths in the water by the experimentation with the intensity parameter. Because the pressure information in different depth are well separated in the dataset, we can easily set different intensity parameters on the 2D transfer function to highlight pressure in different depth, as shown in figure (b)-(d).

3.4 Temperature in electronvolt

We finally rendered the tev dataset. Because we have shown the evolution of v02 and v03, therefore, we only show a demonstration of temperature distribution at time 14533 of yB31 dataset. From figure 3.5 we can see that the highest temperature is only concentrated on the surface of water, which corresponds to the impact region, and the profile of temperature distribution is similar to asteroid. The reason is that the asteroid just impact the water at that time, and the energy has not been transferred to other places.

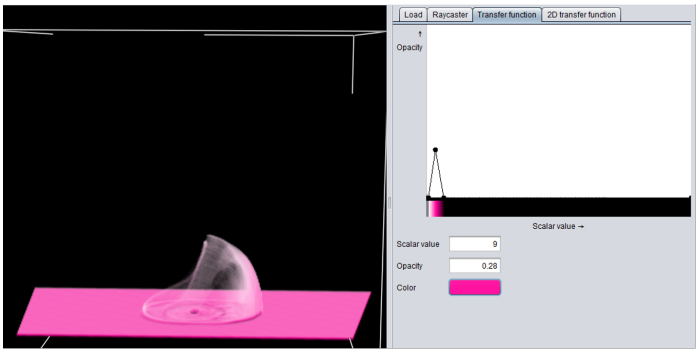

(a)

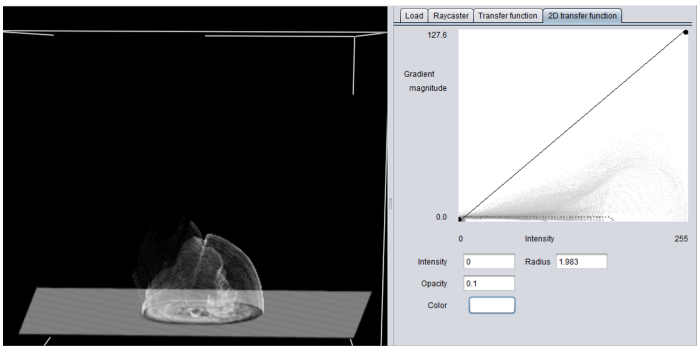

(b)

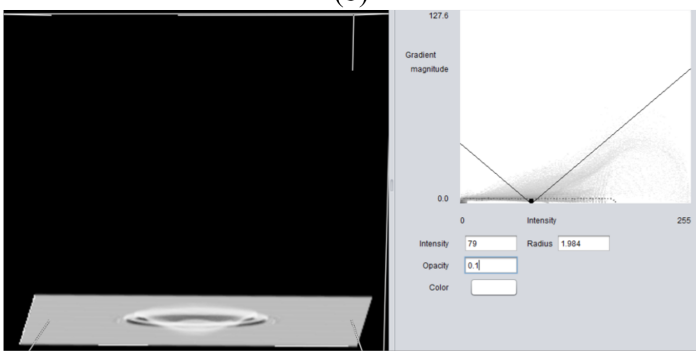

(c)

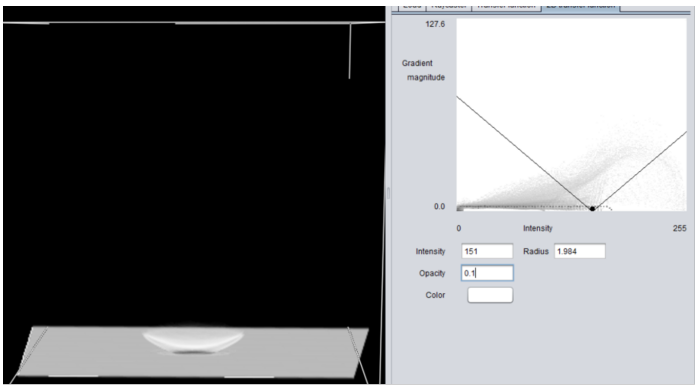

(d)

Figure 3.4: Rendering results of pressure at time 14533 using compositing (figure 3.4(a)) and 2D transfer function method (figure 3.4(b)-(d)). In the 2D transfer functions, the intensity parameters are 0, 79 and 151, the overall opacity and radius are 0.1 and 1.984.

3.4. Temperature in electronvolt

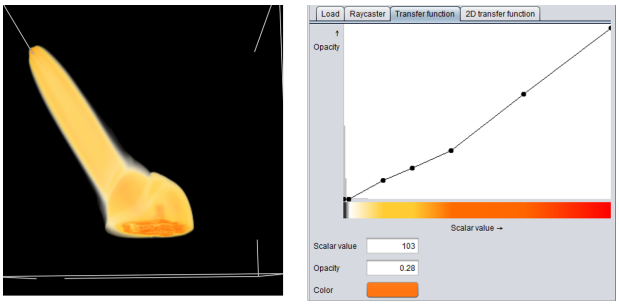

(a) (b)

Figure 3.5: Rendering results of temperature and the corresponding transfer function

Chapter 4

Evaluation

In this chapter, we compare the differences of three volume rendering techniques using theoretical explanations and results analysis. The advantages and disadvantages of each method will be discussed.

4.1 MIP

Maximum ontensity projection is a volume rendering technique for 3D dataset that usually used to depict highest intensity voxels. Compared with compositing and 2D transfer function, the advantage of MIP is that it is convenient and useful to see the inside structure, especially when the inside of objects have a higher intensity than the outside structure. The disadvantages is that MIP lose the information of layers and have no ability to distinguish the spatial details of the surrounding structure and the highest intensity voxels may be from very dense structures, and these structures can obscure the parts that needs to be visualized. In addition, MIP cannot set parameters and colors to present the data.
As seen in figure 1.3, it worked well when we use MIP technique for dataset of backpack and fish, and it showed the pressure wave in the water clearly (figure 3.3). However, it did not work well to see the inside of pig or to view the tomato.

4.2 Compositing

The compositing method can show many details of both outside and inside of the dataset. It can be used to see through layers that have low opacity, while not losing the fact that the layer still exists. The color of each layer which is passed through will stay in the final pixel, and the closer the layer is to the view plane the more its effect will be. This is unlike MIP, since it loses the information of layers. The main advantage of the composite transfer function is that it combines the layers such that no information is lost, but the objects behind some layer are still visible. Also, compositing method can highlight different things of the object by different colors or highlight the part that we

want by setting the opacity of other data points to 0. The disadvantage of compositing is that it shows less information of boundary compared with 2D transfer function.
As seen in figure 1.4, compositing delivers more sophisticated images of fish compared to MIP, it can also show the bone, skin and surrounding of fish separately. MIP only uses one value along the ray, while compositing uses all the values with respect to its alpha value along the ray, and combining them to a single color.

4.3 2D transfer function

2D transfer function is a technique that is very useful when the data sets contain several well separated materials, and it shows more information of boundary than compositing method. Using 2D transfer function, each material type can be separately highlighted easily. However, When voxel values are not well separated, 2D transfer function will not work. In our examples of tooth (figure 2.1), we could easily visualize the tooth head without visualizing any other parts. Another benefit of 2D transfer function is that it allows us to present more features than 1D transfer function, expecially the boundary information. As seen in figure 3.4 (a), the shape and boundary of the pressure shock wave is shown clearer than figure 3.4(b), which means 2D transfer function presents more features of boundary. In general, 2D transfer function gives us more flexibility and possibilities. The disadvantage of 2D transfer function is that it is less flexible of parameters and color setting than compositing.